Analysis of Membrane Protein Self-Association in Lipid Systems by Fluorescence Particle Counting: Application to the Dihydropyridine Receptor[†]

Peter Hinterdorfer,[‡] Hermann J. Gruber,[‡] Jörg Striessnig,[§] Hartmut Glossmann,[§] and Hansgeorg Schindler*[,‡]

Institute for Biophysics, University of Linz, A-4040 Linz, Austria, and Institute for Biochemical Pharmacology, University of Innsbruck, A-6020 Innsbruck, Austria

Received August 12, 1996; Revised Manuscript Received December 10, 1996[⊗]

ABSTRACT: Fluorescence particle counting (FPC) is employed to analyze the distribution of a purified membrane protein, the dihydropyridine receptor (DHP-R), in detergent micelles, in lipid vesicles, and in lipid monolayers generated from the vesicles. The method was used to identify conditions for which DHP-Rs occur singly distributed in micelles and in vesicles. In monolayers, the DHP-R showed self-association, starting from monomeric distribution at concentrations (c) of typically 10 DHP-R/μm^2. The average cluster size [$m(t)$] of associates was followed by FPC in time and the dependence of the lateral diffusion constant [$D_{lat}(m,\pi)$] of the associates on the surface pressure (π) was determined. By studying the dependence of $m(t)$ on c, π, $D_{lat}(\pi)$, and salt concentration (c_s), we derived an empirical expression for the association rate constant (k_a) and for $m(t)$ that fits the experimental $m(t)$ relations. Theoretical justification for these dependencies is obtained from collision theory, leading to a mechanistic picture of the aggregation process. DHP-R association is irreversible. Its rate is not diffusion-limited. A large number of collisions is required to overcome an interaction energy barrier of about 6−11 kT, depending on m and c_s but not on π. The increase in association rate with increasing average cluster size m is related to increasing van der Waals attraction, while the increase in rate with increasing c_s relates to decreasing electrostatic repulsion. Van der Waals and electrostatic forces represent, however, only part of the interaction energy. The main contribution was not dependent on the variables studied and, most likely, reflects hydration forces which need to be overcome for association.

Biological membranes, although they are considered as continuous two-dimensional fluids, are highly heterogeneous with respect to protein distribution, protein mobility, fixation, and clustering. They are particularly designed for functioning in a concerted spatially and temporarily organized way. One clue to the current understanding was the extensive study of protein mobility by fluorescence recovery after photobleaching [FRAP; for reviews see Edidin (1992) and Jacobson et al. (1995)] and high-resolution imaging techniques such as confocal microscopy (Kubitschek et al., 1996) and scanning near-field optical microscopy (SNOM; Betzig et al., 1992; Hwang et al., 1995). This is complemented by single particle tracking, (SPT; Geerts et al., 1987), designed to resolve short-range protein mobility, microheterogeneity, and clustering within discrete and functionally significant domains. In this technique the pathway of individual membrane proteins tagged with beads (Kusumi et al., 1993; Sako et al., 1995) or fluorophores (Gosh et al., 1994) can be followed with nanoscale resolution. The high sensitivity of this method allows one to detect (Funatsu et al., 1995) and track biomolecules carrying only one fluorophore, as shown in lipid membranes (Schmidt et al., 1995, 1996) or along filamentous macromolecules (Sase et al., 1995; Vale et al., 1996).

With increasing phenomenological knowledge about membrane protein morphology and dynamics, a variety of questions arise about mechanism and physical forces governing protein organization. It is, for example, generally unknown whether or to which extent particular protein aggregates are stabilized by extra membrane components or (and) by intramembrane interactions. In this situation it appears profitable to resort to studies of protein interactions in model phospholipid membrane systems. Even then, however, there is a lack of techniques with sufficient time resolution and sensitivity to simultaneously follow protein association and diffusion at appropriately low densities and under conditions relevant to draw mechanistic conclusions. In the present study we analyze the potential of fluorescence particle counting (FPC)[1] (Meyer & Schindler, 1988), a technique particularly designed for the mechanistic study of membrane protein self-association. The measuring principle of FPC [first reported by Weissman et al. (1976)] is similar to that of fluctuation correlation spectroscopy (FCS) (Elson & Magde, 1974; Elson et al., 1975; Magde et al., 1978; Thompson, 1991; Rigler et al., 1992). Applications include the study of the distribution of receptors (Peterson et al., 1993) and IgE molecules (Hwang et al., 1996) in membranes. Recently, two-photon correlation spectroscopy was used to follow diffusion and aggregation of proteins in solution (Berland et al., 1995, 1996).

In FPC, the laser beam is scanned across the sample and fluctuations of the fluorescence signal in space and time are used for the simultaneous determination of aggregation and

[†] This work was supported by the Austrian Research Funds, Projects S/45-01,-03 and S/66-01,-07.

* To whom correspondence should be addressed.

[‡] University of Linz.

[§] University of Innsbruck.

[⊗] Abstract published in *Advance ACS Abstracts,* March 15, 1997.

[1] Abbreviations: DHP-R, dihydropyridine receptor, FPC, fluorescence particle counting.

S0006-2960(96)02009-0 CCC: $14.00

diffusion in 2- and 3-dimensional systems. The protein investigated here is the heterooligomeric ($\alpha 1$, $\alpha 2$-δ, β, γ) dihydropyridine receptor (DHP-R), which constitutes the L-type Ca^{2+} channel, the voltage sensor for excitation−contraction coupling in heart and skeletal muscle [for a review see Glossmann and Striessnig (1990)]. There are indications that L-type Ca^{2+} channels cluster to form "Ca^{2+} hot spots" which induce morphological changes in neuronal growth cones (Silver et al., 1990) and that DHP-R tetramers are colocalized (Flucher et al., 1994) and/or associated with the ryanodine receptor homotetramer, constituting the Ca^{2+} release channel of sarcoplasmic reticulum of skeletal muscle (Block et al., 1988; Hymel et al., 1988a). Furthermore, the voltage-sensor function of the channel may require DHP-R association as evidenced from reconstitution studies in our laboratory (Hymel et al., 1988b). It was the aim of the present study to provide direct evidence for DHP-R association in model membranes and to analyze the association process.

FPC is, in principle, applicable to any lipid/protein model system to monitor protein distribution and redistributions as shown in this work for micelles and vesicles. For a detailed mechanistic study it is required, however, to carry out the study of protein association on single homogeneous membranes with defined initial protein distributions. We have chosen lipid/protein monolayers for this study. This system is favorable as it has been shown (Schürholz & Schindler, 1988) that lipid/protein monolayers with defined lipid/protein ratios can be generated from lipid/protein vesicles without protein denaturation (spreading of vesicles at constant and high surface pressure). With this method different membrane proteins were found to be incorporated in stable form. It was concluded that a hydration layer of water and possibly a lipid shell is bound to the part of the protein in the monolayer that is exposed to the air and prevents unfolding (Schürholz & Schindler, 1988). Moreover, monolayers allow control of system variables relevant for protein association, in conjunction with FPC. We arrive at a rather detailed mechanistic picture for DHP-R association.

MATERIALS AND METHODS

Materials

Soybean lipid (SBL) was obtained from Sigma (Type II-s) and was partially purified by washing in acetone.

Soluble digitonin was prepared by heating a 2% (w/v) solution of digitonin at 90 °C for 1 h. Insoluble material was removed by centrifugation in an ultracentrifuge after the solution was kept at 4 °C for 7 days. WGA-Sepharose was prepared as described (Cuatrecasas & Parikh, 1974). FLUOS (5- and 6-carboxyfluorescein, succinimide ester) was purchased from Molecular Probes, Eugene, OR.

Buffers. *Buffer A* contained 20 mM phosphate, 150 mM NaCl (pH = 7.4), 0.1% digitonin, 0.1 mM PMSF (phenylmethanesulfonyl fluoride), 0.1 mM benzamidine, 1 mM iodoacetamide, and 1 μM pepstatin A. *RB* contained 1 M boric acid, pH = 8.6 (NaOH), and 1.2 mg/mL HTAB (hexadecyltrimethylammonium bromide). *WGA-B1* contained 20 mM phosphate, 150 mM NaCl (pH = 7.0), and 0.1% digitonin. *WGA-B2* was WGA-B1 with 30 mg/mL *N*-acetyl-D-glucosamine. *Buffer B* contained 20 mM phosphate and 350 mM NaCl (pH = 7.0).

All FPC monolayer experiments were done with phosphate buffer except the experiments with Ca^{2+}, where Tris was used.

Methods

All steps during purification, labeling, and vesicle preparation were done at 4 °C. FPC experiments were carried out at room temperature.

Protein Purification and Labeling. DHP-R from rabbit skeletal muscle was highly purified by lectin chromatography and sucrose gradient centrifugation as described in Striessnig et al. (1986) and Striessnig and Glossmann (1991) and stored in liquid nitrogen until use.

For dye conjugation, 0.3 mL of 3 mg/mL FLUOS in buffer RB was added to 1.6 mL of about 20 μg/mL highly purified DHP-R in buffer A and incubated at 4 °C for 3 h with stirring. Then the sample was loaded onto a 1-mL packed volume WGA-Sepharose column equilibrated in buffer WGA-B1. The column was washed thoroughly with 100 mL of the same buffer at a flow rate of 0.25 mL/min to remove the unbound dye. FLUOS-DHP-R was eluted with buffer WGA-B2 and collected in 1-mL fractions with a Bio-Rad Model 2110 fraction collector. Peak fractions (#2 and #3) were pooled, divided into 0.2-mL aliquots, and immediately stored in liquid nitrogen.

Protein concentrations were determined as described in Bradford (1976). Fluorescence was measured in a Shimadzu RF-540 spectrofluorometer with FLUOS as standard and the molecular weight of the DHP-R was taken as MW = 426 000, according to Caterall (1988). This resulted in a labeling stoichiometry of 3.8 ± 0.5 mol of FLUOS/mol of DHP-R (n = 3).

Vesicle Preparation. FLUOS-DHP-R (0.2-mL sample) was added to 0.8 mL of CHAPS−SBL solution with final concentrations of 20 mM phosphate, 350 mM NaCl, pH = 7.0, ~2 μg/mL FLUOS-DHP-R, 0.2 mg/mL digitonin, 6 mg/mL CHAPS, and 3 mg/mL SBL. For detergent removal the sample was gently rotated for 2 × 1 h with 2 × 0.3 mL of Bio-Beads (obtained from Bio-Rad, Richmond, CA). This resulted in vesicles of about 40-nm diameter, which was estimated with a calibrated S-1000 column. Vesicles were then extruded (Lipex Biomembranes Inc., Vancouver, Canada) through a double layer of PC (polycarbonate) membranes with 30-nm pore size to obtain unilamellar vesicles of defined diameter (Hope et al., 1985).

Monolayer Formation. A 0.5-mL sample of 3 mg/mL vesicle suspension (in 20 mM phosphate and 350 mM NaCl) with different protein concentrations (0.05−2 μg/mL) was distributed at the surface of a sand-blasted glass slide (A = 70 cm^2) where a monolayer with high surface pressure (π ~ 25 mN/m) immediately self-assembles. The glass slide was inserted at one end of a Teflon trough with about the same area (A = 70 cm^2) and surface-film formation inside the trough was measured with a Wilhelmy balance. A surface pressure of $\pi \geq 15$ mN/m, where protein denaturation occurs only slowly (Schürholz & Schindler, 1991), was reached within seconds. During FPC measurements the surface pressure was held at least at π = 20 mN/m. The amount of vesicles adsorbed to the monolayer was directly estimated with FPC and found to be very low (<1 vesicle/100 μm^2), not influencing protein aggregation measurements.

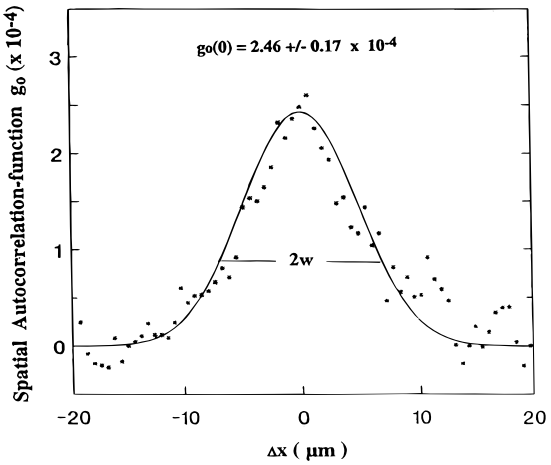

FIGURE 1: Spatial correlation of protein distribution in detergent/protein micelles. For 1.92 μg/mL DHP-R in 1 mg/mL digitonin, the spatial protein distribution is reflected by the spatial autocorrelation function $g_0(x)$ shown, obtained from FPC as previously described (Meyer & Schindler, 1988). The peak value $g_0(0)$ is equal to the reciprocal value of the average number N_p of particles in the illuminated area πw^2. The solid line is a Gaussian distribution with $1/e$ width w (equal to the $1/e^2$ radius of the Gaussian laser beam), known from independent calibration using fluorescence-labeled latex beads. Peak heights yields the $g_0(0) \pm \delta g_0(0)$ value as shown.

FPC Experiments. The FPC machine for particle density and diffusion measurements has been described in detail (Meyer & Schindler, 1988) and was used with the following modifications: (i) For experiments in solution the sample was sucked into a quartz flowthrough cell (Hellma, Bad Mühlheim, Germany) with (10 ± 1)-μm optical pathway, which allowed consecutive measurements without cleaning the cell. (ii) Convection in monolayer experiments could be prevented by inserting a covered Teflon ring with outlet around the quartz lens. For the whole range of conditions for monolayer formation, a time period of 7 ± 0.5 min after inserting the glass slide was found to be sufficient to start FPC experiments. The time scale used in Figures 2−4 and in eq 5 starts at the first measurement.

The width of the Gaussian excitation profile in the sample cell was determined with fluorescent latex beads from the width of the spatial autocorrelation function $g_0(x)$ [see Meyer and Schindler (1988)].

RESULTS

DHP-R Cluster Size in Micelles and in Vesicles. The DHP-R purification procedure used yields the heterooligomeric complex dispersed in aqueous solution by the detergent digitonin. FPC was employed to test whether the DHP-R is well dispersed as monomer or whether it is aggregated. The FLUOS-labeled DHP-R was added to the flowthrough measuring cell at a typical volume concentration c_3 of about 1 DHP-R/μm^3 in the presence of 0.1% digitonin. Figure 1 shows a typical result obtained. FPC measures the autocorrelation function $g_0(x)$ of spatial fluctuations of fluorescence during the cyclic movement of the exciting laser beam. Since the laser beam had a Gaussian intensity distribution with a $1/e^2$ width $w = 6.9$ μm (see Methods section), $g_0(x)$ is expected to be also Gaussian-distributed with w as $1/e$ width (Meyer & Schindler, 1988). Thus, experimental $g_0(x)$ distributions were fitted to Gaussian distributions of given width $2w$; see Figure 1. This yields a peak value $g_0(0) \pm \text{SD} = (2.46 \pm 0.17) \times 10^{-4}$. $1/g_0(0)$ is equal to the average number of independent particles N_p in the illuminated volume $\pi w^2 h$ (h = optical path length of the cell, equal to 10 μm). The average number m of DHP-R molecules in DHP-R aggregates (m is henceforth termed the average cluster size) is then given by

$$m = c_3 \pi w^2 h g_0(0) \qquad (1)$$

The data in Figure 1, obtained at a concentration c_3 of 2.7 ± 0.4 DHP-R/μm^3 as determined from three independent Bradford assays, yields $m = (2.7 \pm 0.4)\pi(6.9)^2\ 10\ [(2.46 \pm 0.17) \times 10^{-4}] = 0.99 \pm 0.22$. Two further determinations confirmed this value (Table 1). It is concluded that DHP-R, in the presence of 0.1% digitonin, is dispersed in monomeric form. The labeled DHP-R occurs thus singly distributed in digitonin micelles. No indication for aggregation was found within at least 2 h (at room temperature) after thawing the labeled DHP-R sample stored on liquid nitrogen.

Table 1: Average Cluster Size (m) of DHP-R in Different Lipid/Detergent Configurations

system	configuration	$m \pm \delta m$ (n)
micelle	digitonin/DHP-R	1.02 ± 0.29 (3)
micelle	digitonin/Chaps/SBL[a]/DHP-R	1.22 ± 0.24 (3)
vesicle	SBL/DHP-R	1.05 ± 0.26 (2)
monolayer ($t = 0$)	SBL/DHP-R	1.06 ± 0.23 (8)

[a] Soybean lipid.

Using the same samples, we searched for conditions where detergent removal after addition of lipid leads to single DHP-R monomers in lipid vesicles. As lipid we used soybean lipid throughout this study. Removal of digitonin in the presence of soybean lipid did not result in sufficiently defined vesicles (data not shown). By trial and error with different detergents and methods for detergent removal, conditions were found for preparing defined vesicles (see Methods). When the original DHP-R/digitonin sample was diluted 5 times into a CHAPS/soybean lipid mixture (6 and 3 mg/mL final concentrations in buffer B), FPC analysis revealed that the DHP-R remained dispersed as monomers (see Table 1). From this sample, detergent was then removed in order to form vesicles. FPC revealed that detergent extraction by Bio-Beads and consecutive extrusion reproducibly gave vesicles which contained singly distributed DHP-R molecules (Table 1). These vesicles showed a diameter of 30 nm when analyzed by a calibrated S-1000 column, which corresponds to about 10^4 lipids/vesicle. Since the overall lipid/DHP-R ratio was 1.5×10^6, only one out of about 150 vesicles carried one DHP-R molecule.

Initial Distribution of DHP-R in Lipid Monolayers Generated from Vesicles. The above lipid vesicles with singly occurring DHP-R molecules were spread to monolayers at the air−water interface (for details see Methods section). Conditions were such that the surface pressure developed sufficiently fast to high values (>15 mN/m) at which surface denaturation is unlikely to occur in analogy to studies on other membrane proteins [see Schürholz and Schindler (1991)]. During FPC measurements, monolayers were held at least at 20 mN/m. The average cluster size m of the DHP-R in such monolayers was evaluated using the relation

$$m = c \pi w^2 g_0(0) \qquad (2)$$

where c is the protein surface concentration in units of

DHP-R per square micrometer, determined directly from FPC from the average fluorescence signal after calibration.

The *m* values found in monolayers were initially always close to 1 (Table 1). This provides direct evidence that spreading leads to singly dispersed DHP-R monomers in lipid monolayers when vesicles with singly occurring DHP-R are used.

Association of DHP-R in Lipid Monolayers. The DHP-R in soybean lipid monolayers was generally found to aggregate to clusters with monotonically increasing average size $m(t)$ within the time of analysis (50 min). Each single determination of *m* in the time course lasted about 1 min. The dependence of average cluster size $m(t)$ was followed in dependence on protein concentration *c*, on salt concentration c_s (NaCl and $CaCl_2$), on surface pressure π, and on the lateral diffusion constant $D_{lat}(\pi)$. Representative results for these dependences are shown in Figures 2−4.

The three data curves in Figure 2A were obtained from the same lipid/DHP-R vesicle sample, diluted by addition of different amounts of pure lipid vesicles to give surface concentrations of $c = 41$, 14, and 4 DHP-R/μm^2. The slope, d*m*/d*t*, clearly increases with increasing *c* and also with increasing *m*. The dependence of d*m*/d*t* on *c* is shown in Figure 2B. The data were obtained at a variety of different conditions of salt and surface pressure (see legend to Figure 2B). Each point in Figure 2B represents a comparison of two curves obtained under the same conditions except different *c* values. The ratio of times (t_2/t_1) to reach the same *m* value (between 8 and 20) are plotted against the inverse concentration ratio (c_1/c_2) in log/log representation. Although the data scatter considerably, probably due to intrinsic statistical variations of the aggregation process, they are represented by a mean slope close to 1 with SD of 0.39. This suggests that the association rate $k_a \equiv dm/dt$ is proportinal to the DHP-R monomer concentration *c*.

Figure 3 summarizes results obtained for the dependence of $m(t)$ on the surface pressure π and on the simultaneously measured lateral diffusion constant D_{lat}. The two curves in Figure 3A, measured at quite different π values of 27 (▽) and 43 (○) mN/m, indicate a rather moderate effect of π on the association rate. The dependence of the association rate k_a on surface pressure π was evaluated by measuring the time $t(\pi)$ to reach a certain *m* value ($m = 8$) for different surface pressures. The data were normalized to $\pi = 20$ mN/m and corresponding ratios $t(\pi = 20\ \text{mN/m})/t(\pi)$ are shown in Figure 3B (Δ, right scale). To test whether k_a is directly influenced by the surface pressure π or only via the π dependence of the diffusion coefficient D_{lat}, the value of $D_{lat}(\pi)$ was simultaneously measured (Figure 3B, ○, left scale).[2] The two data sets, for $k_a(\pi)$ and for $D_{lat}(\pi)$, reasonably match. This indicates that there is no significant direct effect of π on DHP-R association rate k_a, only a small indirect effect via $D_{lat}(\pi)$, to which k_a is proportional.

The two results, referrable to Figures 2B and 3B, suggest that

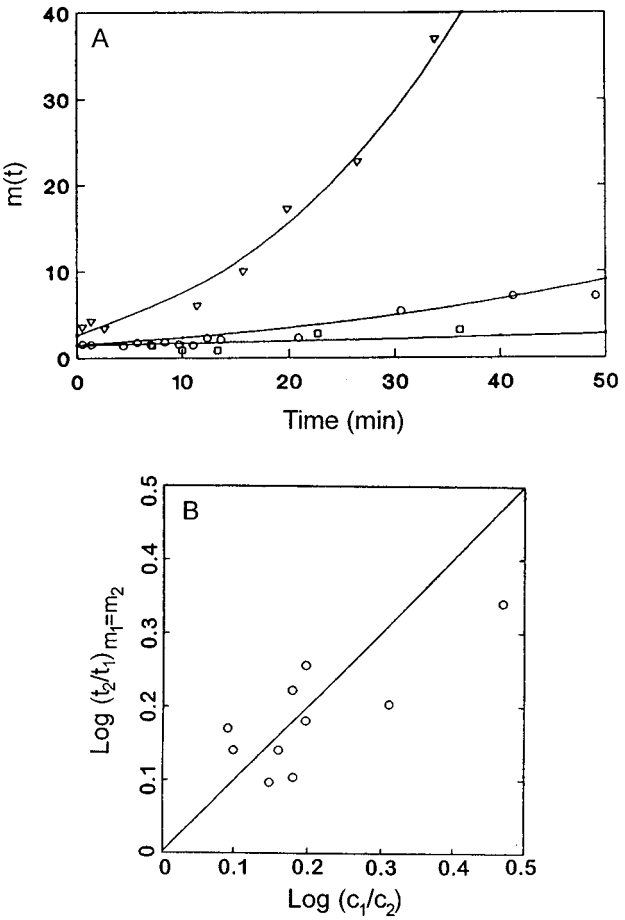

FIGURE 2: Dependence of DHP-R aggregation $m(t)$ on DHP-R surface density *c*. (A) The average cluster size $m(t)$ of the DHP-R in soybean lipid monolayers is followed by repeated measurements of *m* (measuring time about 1 min). Protein concentrations were 4 DHP-R/μm^2 (□), 14 DHP-R/μm^2 (○), and 41 DHP-R/μm^2 (▽). Other variables were constant, surface pressure at 24 ± 1 mN/m and salt concentration 150 mM NaCl. The solid lines were calculated from eq 5 with $z = 3.2$. Protein concentrations used for the calculations were determined independently from the average fluorescence observed, normalized to the fluorescence of one FLUOS molecule. Corresponding D_{lat} values were taken from Figure 3B. Fits yielded $h(c_s)$ values as shown in Table 2. (B) The times to reach the same *m* value ($m = 8$ or 10) are plotted against the concentration ratio (c_1/c_2). For each comparison of the effect of *c* on aggregation rate, the same experimental conditions were used with respect to surface pressure π and salt concentration c_s. The data include comparisons made at $c_s = 0$ and 150 mM NaCl and π values in the range of 20−42 mN/m.

$$k_a \propto cD_{lat}(\pi) \qquad (3)$$

Figure 4 shows that the DHP-R association rate k_a increases with increasing salt concentration, c_s (see panel A for NaCl and panel B for $CaCl_2$). At the highest salt concentrations applied, *m* increases monotonically to values of up to 200, which clearly shows that DPH-R association is irreversible up to very high *m* values. Moreover, the slope $dm/dt = k_a$ increased monotonically with increasing *m* at all conditions applied. This dependence is, within experimental accuracy, well described by a power law, i.e., $k_a \propto m^\gamma$. Based on the data, the empirical expression for k_a reads

$$dm/dt \equiv k_a(m) = cD_{lat}(\pi)\, h(c_s)\, m^\gamma = km^\gamma \qquad (4)$$

The proportionality factor $h(c_s)$ includes empirical dependencies of k_a on the concentration of salts, c_s. Integration of

[2] It may be noted that the D_{lat} values, reported here for the first time for a protein in monolayers, are very close to values reported for proteins in lipid membranes [reviewed by Clegg and Vaz (1985)]. Also, the π dependence of D_{lat} and its *m* dependence (not included here), measurable by FPC, allows theoretical predictions (Saffman & Delbrück, 1975) to be tested.

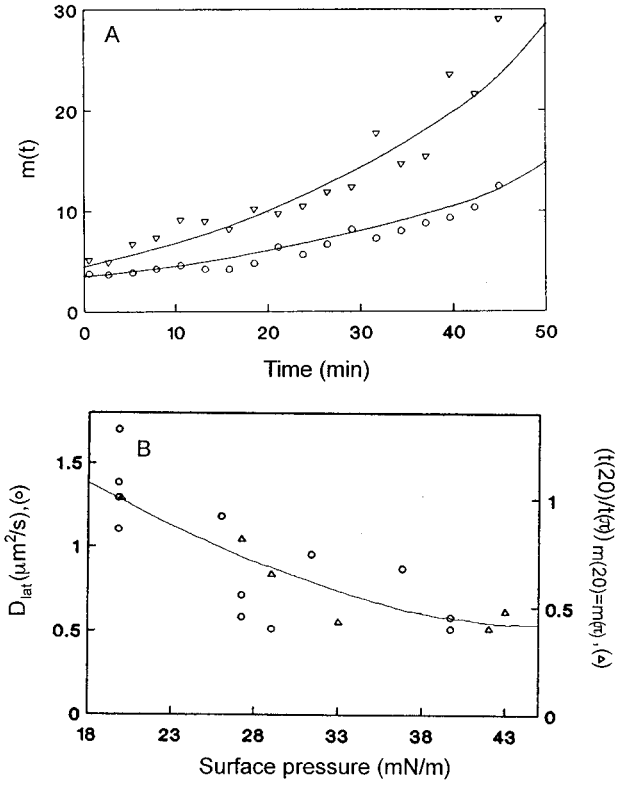

FIGURE 3: Dependence of DHP-R association $m(t)$ on surface pressure π and lateral diffusion constant $D_{lat}(\pi)$. (A) $m(t)$ is shown for a low value of surface pressure $\pi = 27$ mN/m (∇) and for the highest accessible value $\pi = 43$ mN/m (○). For both sets of data c was 47 ± 2 μm^{-2} and no salt had been added to the monolayer buffer (bidistilled water). The solid lines were calculated from eq 5 with $z = 3.2$. (B) Right scale (△) shows the measured times, $t(\pi)$, to reach $m = 8$ plotted against π, normalized to t ($\pi = 20$ mN/m). Simultaneously, the left scale (○) shows the lateral diffusion constant $D_{lat}(\pi, m)$ measured for different π values at constant m ($m = 8 \pm 2$ as average over measuring time for D_{lat}).

eq 4 yields

$$m(t) = (tk/z + m(0)^{1/z})^z \tag{5}$$

with $z = 1/(1 - \gamma)$ and $k = cD_{lat}(\pi)\ h(c_s)$. $m(0)$ is the average cluster size at the start of the FPC experiment (defined as $t = 0$). The solid lines in Figures 2−4 were calculated from eq 5. Such fits yielded two main results: (i) All experimental data could be fitted with virtually the same z, $z = 3.2 \pm 0.5$, corresponding to $\gamma = 0.69 \pm 0.05$. (ii) The factor $h(c_s)$ is a measure for the probability of association upon collision and showed a dependence on salt concentration c_s as seen in Table 2. The tendency in the $h(c_s)$ values is in qualitative agreement with reduction of electrostatic repulsion between associating proteins with increasing salt concentration c_s. It should be noted that even for the highest salt effect observed, at 150 mM NaCl and 2 mM $CaCl_2$, the value of h is much below 1, i.e., $h = (4.17 \pm 0.42) \times 10^{-5}$, referred to as h_{max}.

Together, these findings indicate that the modulation of the association rate k_a by the average cluster size m, DHP-R surface concentration c, monolayer pressure π, and salt concentration c_s can reasonably be accounted for by the empirical equation 4 and the data in Table 2. The influence of these experimental variables on k_a is, however, quite small compared to the influence of h_{max}. The low value of h_{max} indicates an additional high energy barrier for DHP-R association, which is not dependent on the variables studied.

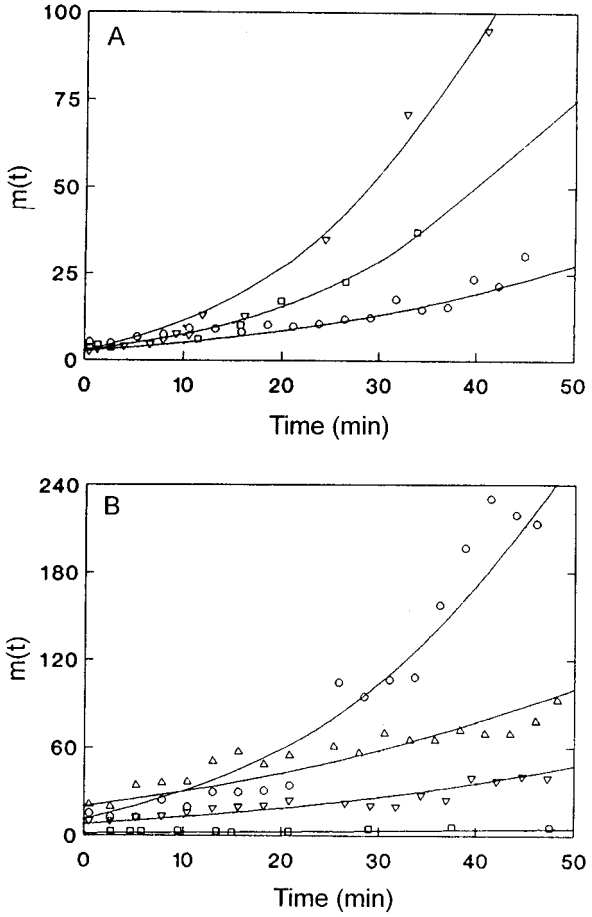

FIGURE 4: Time course of DHP-R aggregation $m(t)$ for different salt conditions. (A) Dependence on NaCl concentration: 650 mM (∇), 150 mM (□), 0 mM (○). The DHP-R surface concentration c was 45 ± 3 μm^{-2} and the surface pressure $\pi = 27 \pm 2$ mN/m. Solid lines were calculated from eq 5 with $z = 3.2$. D_{lat} values were taken from Figure 3B. Fits yielded the values for $h(c_s)$, listed in Table 2, describing the effect of c_s on aggregation rate. (B) Enhancement of aggregation rate by $CaCl_2$. In addition to 150 mM NaCl, $CaCl_2$ was added: 0.1 mM (∇), 0.5 mM (△), and 2 mM (○). For comparison, the lowest curve (□) shows $m(t)$ measured in bidistilled water. Other variables were $c = 28 \pm 3$ μm^{-2} and $\pi = 29 \pm 3$ mN/m. Solid lines were calculated from eq 5 ($z = 3.2$), yielding $h(c_s)$ values listed in Table 2.

Table 2: Effect of Salt on DHP-R Aggregation[a]

NaCl (mM)	$CaCl_2$ (mM)	$h(c_s) \times 10^5$
0	0	0.58 ± 0.08
150	0	1.01 ± 0.17
650	0	1.33 ± 0.21
150	0.1	1.66 ± 0.24
150	0.5	2.01 ± 0.29
150	2	4.17 ± 0.42

[a] This table gives the mean $h(c_s)$ values obtained from fits of the data in Figures 2−4 using eq 5 with known c and D_{lat} values for different salt concentrations $h(c_s)$. The $h(c_s)$ values are a measure for the probability of association upon collision.

DISCUSSION

The rate equations of a reaction scheme for the irreversible formation of clusters

$$A_i + A_j \xrightarrow{k_{ij}} A_{i+j} \tag{6}$$

where A_i denotes clusters with size i and k_{ij} denotes the size-dependent association rate constant, can be described by the Smoluchowsky equation (Meakin, 1990):

$$dc_n/dt = {}^1/_2 \sum_{i+j=n} k_{ij}c_ic_j - c_n\sum_j k_{jn}c_j \quad (7)$$

where c_n is the particle concentration of clusters of size n. The average cluster size m measured by FPC is a mass average and relates to c_n by

$$m = \sum_n n^2c_n/\sum_n nc_n = 1/c(\sum_n n^2c_n) \quad (8)$$

with c as total particle density. The association rate $k_a \equiv dm/dt$ is then deduced from the Smoluchowsky equations according to

$$k_a = dm/dt = 1/c\sum_n n^2\, dc_n/dt = 1/c\sum_n n^2({}^1/_2 \sum_{i+j=n} k_{ij}c_ic_j - c_n\sum_j k_{jn}c_j) \quad (9)$$

For the conditions in this study, low cluster density and low probability for association upon collision, it is justified to use the Smoluchowsky equation approach for $m(t)$ (Kolb, 1984). An analytical expression for $m(t)$ can be found using the scaling form (Kolb, 1984; Vicsek & Family, 1984; Meakin, 1990). The system is at any time at equilibrium with respect to the cluster size distribution, and the time development of the average cluster size $m(t)$ can be described by a single exponent (Kolb, 1984; Vicsek & Family, 1984; Meakin, 1990):

$$m(t) \propto t^z \quad (10)$$

Comparing eq 10 with eq 5, it can be seen that the expression derived for $m(t)$ in eq 5 from the empirical dependencies in the association rate k_a represents the solution of the general Smoluchowsky rate equation with $z = 3.2 \pm 0.5$. The empirically found power law dependence of k_a on m, $k_a \propto m^\gamma$ ($\gamma = 0.69 \pm 0.05$), is consistent with eq 10.

For a discussion of the other variables in k_a, i.e., protein density c, $D_{lat}(\pi)$, and $h(c_s)$, k_a will be compared with predictions from a general theory (Szabo et al., 1980). The required nomenclature is defined in Figure 5. The diffusion of a particle P_1 in two dimensions and its encounters with a particle P_2 can be reduced to diffusion of P_1 within a circle of radius R, containing P_2 at a fixed position. $\pi R^2 = 1/c_{particle} = m/c$ is the average area per particle of average cluster size m. We assume structural relaxation, that is, association of m protomers to a particle P may lead to approximately circular particles of area $\pi a^2 = md^2$ with d^2 as effective area per protomer. The mean encounter time τ for particle collision in an interaction potential $U(r)$ is

$$\tau = D_{lat}\int_a^R 2\pi r_0 \int_a^{r_0} \frac{1}{r} e^{u(r)/kT} \int_r^R x e^{-u(x)/kT}\, dx\, dr\, dr_0 / \int_a^R 2\pi r_0\, dr_0 \quad (11)$$

For $U(r) = 0$ (diffusion-limited reaction), integration gives (Szabo et al., 1980)

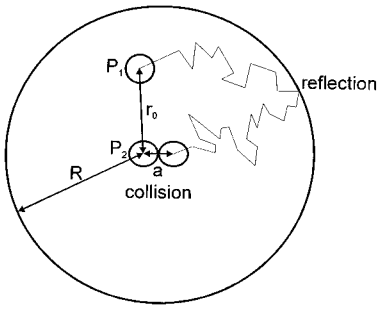

FIGURE 5: Scheme for the definition of variables in the theoretical treatment. Particle diffusion and collision within an ensemble of particles in a two-dimensional system has been shown (Szabo et al., 1980) to be reasonably described by reduction to two particle collisons in a limited diffusion area. One representative particle, P_1, is allowed to diffuse freely within an area πR^2, which is equal to the average area per particle ($\pi R^2 = 1/c_p = m/c$). When the particle starts from a random position (r_0), diffusion may lead to the boundary at R where the particle is reflected. Eventually, it encounters particle P_2 in the center (collision).

$$\tau_0 = \frac{R^2}{4D_{lat}} f(x^2) = \frac{m}{4\pi cD_{lat}} f(x^2) \quad (12)$$

with

$$f(x^2) = \frac{\ln(1/x^2)}{1 - x^2} - \frac{3 - x^2}{2}$$

and

$$x^2 = (a/R)^2 = cd^2$$

yielding an association rate k_0:

$$k_0 = \frac{m}{\tau_0} = 4\pi cD_{lat}/f(x^2) \quad (13)$$

Using typical values for the beginning of the association process, $c \approx 10/\mu m^2$, $D_{lat} = 1\ \mu m^2/s$, and $d \approx 10$ nm for the DHP-R size in the monolayer as estimated from Leung et al. (1988), x^2 is $\sim 10^{-3}$ (area fraction occupied by protein) so that $f(x^2) \approx 5$. This yields $k_0 \approx 25\ s^{-1}$. This rate k_0 is much higher than the k_a values found, indicating that association of DHP-R molecules is not diffusion-limited. The association rate is limited by a high activitation energy barrier $U(r)$ that requires a large number of collisions, n_c, to be overcome, which is estimated to be in the range of

$$n_c = \frac{k_0}{k_a} \approx 6 \times 10^4 \text{ to } 6 \times 10^2 \quad (14)$$

The high and lower values of n_c were calculated from the lowest and highest initial association rates $k_a(t = 0)$ observed, $k_a = 4.22 \times 10^{-4}\ s^{-1}$ at $c_s = 0$ and $k_a = 4.17 \times 10^{-2}\ s^{-1}$ at $c_s = 150$ mM NaCl and 2 mM $CaCl_2$. Using $U_{max}/kT \gg 1$ and $x^2 \ll 1$, valid for the conditions in this study, eq 11 can be well approximated by

$$\tau \approx \frac{m}{2\pi cD_{lat}} \int_{r(U_{max})}^{r(U\approx 0)} r^{-1} e^{u(r)/kT}\, dr \quad (15)$$

so that

$$k_a \approx cD_{lat}2\pi / \int_{r(U_{max})}^{r(U\approx 0)} r^{-1} e^{u(r)/kT}\, dr \quad (16)$$

First, it is to be noted that k_a is proportional to cD_{lat}. This agrees with the experimental finding, as expressed in eqs 4 and 5. From the relation $g_s = h(c_s)/h_{max}$, the other factors in eq 4 are related to $U(r)$ by

$$(h_{max} g_s m^{\gamma})^{-1} = \int_{r(U_{max})}^{r(U\approx 0)} r^{-1} e^{U(r)/kT}\, dr/2\pi \qquad (17)$$

There are at least three main energy contributions to be considered: electrostatic energy U_{es} and hydration energy U_{hyd} giving rise to repulsive forces, reduced by attraction due to van der Waals energy:

$$U = U_{es} + U_{vdw} + U_{hyd} \qquad (18)$$

The observed salt dependence of k_a has been separated by introducing the factor g_s, which describes the reduction of k_a due to electrostatic repulsion. The increase of rate k_a with increasing average cluster size, m, accounted for by m^{γ}, implies increasing attraction with increasing average cluster size m. The finding of $\gamma = 0.69 \pm 0.05 > 0$ is attributed to van der Waals attraction, U_{vdw}. Dependence of U_{es} on m would be of opposite sign ($\gamma_{es} < 0$). During collisions, charges are not sensed beyond a certain distance characterized by the Debye length, which is smaller than or at the most comparable (at zero salt) with the diameter of one DHP-R molecule. London−van der Waals forces are sufficiently long-range to account for a monotonic increase of k_a with m up to the m values measured. The observed irreversibility of DHP-R association is also attributed to van der Waals attraction, governing the potential $U(r)$ for contacting structures. During association, the receptors have to overcome a high activation barrier, mainly attributed to hydration energy U_{hyd}. Even at the fastest rates (at 2 mM $CaCl_2$ and 150 mM NaCl), about 600 collisions are still required to overcome the barrier. In analogy to the elegant work on repulsive forces between membranes [see, e.g., Parsegian et al. (1979) and Horn (1984)], proteins within the monolayer plane should experience strong repulsive hydration forces, originating from the activation energy required for the fusion of the two hydration shells of the colliding particles to a new extent of hydration. Quantitations of these qualitative assignments would require numerical solution of eq 17 with explicit expressions for the three energies, which was not attempted.

Implication of the observed DHP-R association for its function as a voltage-sensing ion channel is provided in combination with previous findings. The DHP-R was shown to form an ion channel in planar lipid bilayers and its channel characteristics have been investigated (Hymel et al., 1988b). The initially linear current−voltage relation of the channels changed in a time, adjustable by DHP-R density, to voltage-dependent gating as found in native skeletal membranes by patch-clamp techniques (Rios & Brum, 1987; Glossman & Striessnig, 1990). It was concluded that the DHP-Rs associate and that this association is required for the voltage-sensor function of the DHP-R in excitation−contraction coupling. Also, electron microscopy of skeletal muscle membranes revealed that the DHP-R and the Ca^{2+} release channel are physically connected (Block et al., 1988). Every second Ca^{2+} release channel is associated with four DHP-R molecules. Thus, the DHP-R association may be the structural counterpart of its functioning as a voltage sensor in excitation−contraction coupling. From the data in the present study it appears that the DHP-R has a genuine tendency to form aggregates in lipid membranes. By interaction with the Ca^{2+} release channel the DHP-R aggregates may be localized and restricted. Finally, it has been shown (Silver et al., 1990) that in neuronal growth cones DHP-Rs are grouped in clusters and cause Ca^{2+} hot spots. In this way enzymes with a micromolar requirement for Ca^{2+} can be activated.

In conclusion, FPC has been applied to measure the average cluster size m of a purified membrane protein, the heterooligomeric dihydropyridine receptor (DHP-R), in typical lipid environments. We found conditions for monomolecular dispersion ($m = 1$) of DHP-R in micelles and lipid vesicles, obtained by detergent extraction. In monolayers generated from DHP-R−lipid vesicles, the DHP-R aggregated to clusters with monotonically increasing size $m(t)$, starting from monomeric distribution. The association rate k_a increased with salt concentration (NaCl and $CaCl_2$) and with increasing average cluster size m and was found to be proportional to the DHP-R surface concentration c and the diffusion constant $D_{lat}(\pi)$. We derived a detailed mechanistic picture of DHP-R aggregation in monolayers. DHP-R aggregation is not diffusion-limited. There are at least three main interaction energy contributions: electrostatic and hydration energy giving rise to repulsion and van der Waals energy giving rise to attraction. Aggregation is irreversible due to van der Waals attraction which dominates the interaction between DHP-Rs at sufficiently close approach. For association, many collisions (up to 6×10^4) are needed, corresponding to a high energy barrier (up to 11 kT), most likely due to strong repulsive hydration forces. The DHP-R association has functional implications in excitation−contraction coupling and neurons.

ACKNOWLEDGMENT

We are grateful to Dr. V. Pastushenko for computer calculations and to A. Schurga and C. Eiter for expert technical assistance.

REFERENCES

Berland, K. M., So, P. T. C., & Gratton, E. (1995) *Biophys. J. 68*, 694−701.

Berland, K. M., So, P. T. C., Chen, Y., Mantulin, W. W., & Gratton, E. (1996) *Biophys. J. 71*, 410−420.

Betzig, E., & Trautmann, J. K. (1992) *Science 257*, 189−195.

Block, B. A., Imagawa, T., Campbell, K. P., & Franzini-Armstrong, C. (1988) *J. Cell Biol. 107*, 2587−2600.

Bradford, M. M. (1976) *Anal. Biochem. 72*, 248−254.

Catterall, W. A. (1988) *Science 242*, 50−61.

Clegg, R. M., & Vaz, V. L. C. (1985) in *Progress in Protein−Lipid Interactions* (Watts, A., & De Pont, J. J. H. H. M., Eds.) pp 173−229, Elsevier Science Publisher B. V., Amsterdam, The Netherlands.

Cuatrecasas, P., & Parikh, I. (1974) *Methods Enzymol. 34*, 653−670.

Edidin, M. (1992) in *The Structure of Biological Membranes* (Yeagle, P., Ed.) pp 539−572, CRC Press, Boca Raton, FL.

Elson, E. L., & Magde, D. (1974) *Biopolymers 13*, 1−27.

Elson, E. L., Magde, D., & Webb, W. W. (1974) *Biopolymers 13*, 29−61.

Flucher, B. E., Andrews, S. B., & Daniels, M. P. (1994) *Mol. Biol. Cell 5*, 1105−1118.

Funatsu, T., Harada, Y., Tokunaga, M., Saito, K., & Yanagida, T. (1995) *Nature 374*, 555−559.

Glossmann, H., & Striessnig, J. (1990) *Rev. Physiol. Biochem. Pharmacol. 114*, 1−105.
Gosh, R. N., & Webb, W. W. (1994) *Biophys. J. 66*, 1301−1318.
Hope, M. J., Bally, M. B., Weble, G., & Cullis, P. R. (1985) *Biochim. Biophys. Acta 812*, 55−65.
Horn, R. G. (1984) *Biochim. Biophys. Acta 778*, 224−228.
Huang, Z., & Thompson, N. L. (1996) *Biophys. J. 70*, 2001−2007.
Hwang, J., Tamm, L. K., Böhm, C., Ramalingam, T. S., Betzig, E., & Edidin, M. (1995) *Science 270*, 611−614.
Hymel, L., Inui, M., Fleischer, S., & Schindler, H. (1988a) *Proc. Natl. Acad. Sci. U.S.A. 85*, 441−445.
Hymel, L., Striessnig, J., Glossmann, H., & Schindler, H. (1988b) *Proc. Natl. Acad. Sci. U.S.A. 85*, 4290−4294.
Jacobson, K., Sheets, D. E., & Simson, R. (1995) *Science 268*, 1441−1442.
Kolb, M. (1984) *Phys. Rev. Lett. 53*, 1653−1656.
Kubitschek, U., Wedekind, P., Zeidler, O., Grote, M., & Peters, R. (1996) *Biophys. J. 70*, 2067−2077.
Kusumi, A., Sako, Y., & Yamamoto, M. (1993) *Biophys. J. 65*, 2021−2040.
Leung, A. T., Imagawa, T., Block, B., Franzini-Armstrong, C., & Campbell, K. P. (1988) *J. Biol. Chem. 263*, 994−1001.
Magde, M., Webb, W. W., & Elson, E. L. (1978) *Biopolymers 17*, 361−376.
Meakin, P. (1990) *Physica A 165*, 1−18.
Meyer, T., & Schindler, H. (1988) *Biophys. J. 54*, 983−993.
Parsegian, V. A., Fuller, N., & Rand, R. P. (1979) *Proc. Natl. Acad. Sci. U.S.A. 76*, 2750−2754.
Petersen, N. O., Hoddelius, P. L., Wiseman, P. W., Seger, O., & Magnusson, K. E. (1993) *Biophys. J. 65*, 1135−1146.
Rigler, R., Wildgren, J., & Mets, U. (1992) in *Fluorescence Spectroscopy: New Methods and Applications* (Wolfbeis, I. S., Ed.) pp 13−24, Springer, New York.
Rios, E. & Brum, G. (1987) *Nature 325*, 717−720.
Saffmann, P. G., & Delbrück, M. (1975) *Proc. Natl. Acad. Sci. U.S.A. 72*, 3111−3113.
Sako, Y., & Kusumi, A. (1995) *J. Cell Biol. 129*, 1559−1574.
Sase, I., Miyata, H., Corrie, J. E. T., Craik, J. S., & Kinosita, K., Jr. (1995) *Biophys. J. 69*, 323−328.
Schmidt, Th., Schütz, G. J., Baumgartner, W., Gruber, H. J., & Schindler, H. (1995) *J. Phys. Chem. 99*, 17662−17668.
Schmidt, Th., Schütz, G. J., Baumgartner, W., Gruber, H. J., & Schindler, H. (1996) *Proc. Natl. Acad. Sci. U.S.A. 93*, 2926−2929.
Schürholz, Th., & Schindler, H. (1988) *Biophys. J. 54*, 983−993.
Schürholz, Th., & Schindler, H. (1991) *Eur. Biophys. J. 20*, 71−81.
Silver, A. R., Lamb, A. G., & Bolsover, S. R. (1990) *Nature 343*, 751−754.
Striessnig, J., & Glossmann, H. (1991) *Methods Neurosci. 4*, 210−222.
Striessnig, J., Moosburger, K., Goll, A., Ferry, D. R., & Glossmann, H. (1986) *Eur. J. Biochem. 161*, 603−609.
Szabo, A., Schulten, K., & Schulten, Z. (1980) *J. Chem. Phys. 72*, 4350−4357.
Thompson, N. L. (1991) in *Topics in Fluorescence Spectroscopy 1: Techniques* (Lakowicz, J. R., Ed.) pp 337−378, Plenum, New York.
Vale, R. D., Funatsu, T., Pierce, D. W., Romberg, L., Harada, Y., & Yanagida, T. (1996) *Nature 380*, 451−453.
Vicsek, T., & Family, F. (1984) *Phys. Rev. Lett. 52*, 1669−1672.
Weissman, M., Schindler, H., & Feher, G. (1976) *Proc. Natl. Acad. Sci. U.S.A. 73*, 2776−2780.
Wong, J., & Pullman, A. (1991) *Biochim. Biophys. Acta 1070*, 493−496.

BI962009C